Contents list available at IJRED website

Int. Journal of Renewable Energy Development (IJRED)

Journal homepage: https://ijred.undip.ac.id

Research Article

Au Nanoparticles Effect on Inverted ZnO Nanorods/Organic Hybrid Solar Cell Performance

Pham Hoai Phuong[a*], Kang Jea Lee[a], Huynh Tran My Hoa[a], Hoang Hung Nguyen[a], Quang Trung Tran[b], Nguyen Thi Hai Yen[c], Tran Viet Cuong[a*]

[a]*VKTECH Research Center, Nguyen Tat Thanh University, 298-300A Nguyen Tat Thanh Street, Ward 13, District 4, Ho Chi Minh City, Vietnam*

[b]*Department of Solid State Physics, University of Science, Vietnam National University-Ho Chi Minh City (VNU-HCM), 227 Nguyen Van Cu, Ward 4, District 5, Ho Chi Minh City, Vietnam*

[c]*Faculty of Science, Dong Nai University, 4 Le Quy Don Street, Tan Hiep Ward, Bien Hoa City 76111, Vietnam*

Abstract. The sun provides a plentiful and inexpensive source of carbon-neutral energy that has yet to be fully utilized. This is a major driving force behind the development of organic photovoltaic (OPV) materials and devices, which are expected to offer benefits such as low cost, flexibility, and widespread availability. For the photovoltaic performance enhancement of the inverted ZnO-nanorods (NR)/organic hybrid solar cells with poly(3-exylthiophene):(6,6)-phenyl-C61-butyric-acid-methylester (P3HT:PCBM) and poly (3,4-ethylenedioxythiophene):poly (styrenesulfonate) (PEDOT:PSS) active layers, gold nanoparticles (Au-NPs) were introduced into the interface between indium-thin-oxide cathode layer and ZnO cathode buffer layer, and the efficiency improvement was observed. It's worth noting that adding Au NPs had both a positive and negative impact on device performance. Au NPs were shown to be advantageous to localized surface plasmon resonance (LSPs) in the coupling of dispersed light from ZnO NRs in order to extend the light's path length in the absorbing medium. Although the light absorption in the active layer could be enhanced, Au NPs might also act as recombination centers within the active layer. To avoid this adverse effect, Au NPs are covered by the ZnO seeded layer to prevent Au NPs from direct contact with the active layer. The dominant surface plasmonic effect of Au NPs increased the photoelectric conversion efficiency from 2.4% to 3.8%.

Keywords: Organic solar cells, gold nanoparticles, localized surface Plasmon

Article history: Received: 3rd Aug 2021; Revised: 18th Oct 2021; Accepted: 26th Oct 2021; Available online: 4th Nov 2021
How to cite this article: Phuong, P.H., Lee, K.J., Hoa, H.T.M., Nguyen, H.H., Yen, N.T.H., Tran, Q. T, and Cuong. V.T, D. (2022) Au Nanoparticles Effect on Inverted ZnO Nanorods/Organic Hybrid Solar Cell Performance. *Int. J. Renew. En. Dev.,* 11(1), 165-171
https://doi.org/10.14710/ijred.2022.40492

1. Introduction

Solar energy could be a reliable solution without any supply limit to the hazardous problems of climate change and environmental contaminations caused by global warming gases from the burning of fossil fuels. Consequently, converting the energy of light directly into electricity by means of photovoltaics (PVs) becomes one of the most pertinent research topics nowadays. The demand for fundamentally new technologies of PVs stimulated scientific research to develop high efficient solar cells. Throughout the past decades, PVs technology has been introduced and developed commercially in field of crystalline Si-based solar cells with power conversion efficiencies (PCE) as ~25.6%. In particular, a mono-crystalline GaAs based PVs devices have been manufactured with maximum PEC performance being about 28.8% for mono-junctions and 37.9% for multi-junction standem cells (Green *et al*., 2014). However, the global use of solid semiconductor-based solar cells is emerging at a slow pace. The reason behind this is high cost and low mass-production capability of mono-crystalline semiconductor-based solar cells. Despite the technology advancement which resulted in a remarkable price drop of solid-state PVs devices, the cost is still unaffordable as compared to that of current energy sources. Moreover, the manufacturing process often leads to lower efficiency due to the formation of contaminants and invasive chemicals. The inflexibility is another challenge, which prevents large scale installations.

In comparison with the currently dominating solid-state Si and compound semiconductor-based devices, the organic PVs have the potential to contribute significantly to the solar energy market due to their many favorable properties including ease of processing, low-cost, low-temperature fabrication, light-weight, optical tenability, semi-transparency, portability, mechanical flexibility and substantial ecological benefits (Kaltenbrunner *et al*., 2012). Moreover, organic solar cells could be printed out using an inkjet printer resulting in flexible and roll-to-roll

* Corresponding author: phphuong@ntt.edu.vn; tvcuong@ntt.edu.vn

devices (Krebs, 2009). From the first bilayer organic solar cells was developed by Tang *et al* (Tang *et al.*, 2014), a lot of attempts have been made in order to overcome the drawbacks of increasing the performance of these devices. However, organic devices are still far behind their inorganic counterparts considering their low performance. The organic based PVs devices could be fabricated with a very thin layer of active material due to their high optical absorption coefficient and the organic solar cells possess quite lower efficiencies than their solid-state semiconductor counterparts. The most recent reported PCE of organic solar cells is around 7.4% (Liang *et al.*, 2010). The low charge carrier mobility and charge collection properties, as well as the mismatch between the absorption spectra of the device and the solar radiation, could be mentioned as some of the principal obstacles to achieve highly efficient organic solar cells. Morphology-dependent charge transport properties, long-term stability, light-harvesting limitations, photocurrent, and efficiency are still the remaining issues at the center of scientific attention in the organic solar cells field. To commercialize the organic solar cells, higher light-harvesting efficiencies will be required. Over the years, the performance of standard typical devices enhanced remarkably by various design, material, structure and morphology manipulations such as the development of bulk heterojunction active layer instead of bilayer structure (Yu *et al.* 2004, Hoppe *et al.* 2004), taking advantage of various buffer layers and metal electrodes (Brabec *et al.*, 2002),(Eo *et al.*, 2009),(Alem *et al.*, 2013), using different active layer materials with different concentrations (Alem *et al.*, 2004), and introduction of nanostructure hybrid (Jagadeesh *et al.*, 2014) and tandem solar cells (Ameri *et al.*, 2009). However, new technologies should be developed in order to improve the performance of organic solar cells.

One recent approach is the incorporation of noble metallic nanoparticles (NPs) in organic solar cells which could significantly contribute to the wave nature of light as resonance through surface plasmons excited at metallic nanostructures. In particular, the most notable phenomenon occurring with the metal nano-structures is electromagnetic resonances due to collective charge oscillations of the metal's free electrons, termed localized surface plasmons (LSPs) and surface plasmon polaritons (SPPs). Due to their unique optical and electronic properties, plasmonic metal thin-films and NPs were proposed to improve the performance of many optoelectronic devices based on resonance interactions of surface plasmon with incident light or with excited states of attached functional molecules. Application of noble metallic NPs was suggested also as one of the possible ways of increasing the power conversion efficiency of PVs devices (Gu *et al.*, 2012). The plasmonic features have attracted interest for the enhancement of light harvesting capacity by resonance trapping the light in the active layer of organic solar cells with metallic NPs, i.e. Ag or Au nano-materials (Lu *et al.*, 2012),(Hwang *et al.*, 2009). Also, there have been multiple studies for plasmonic effects of Au-NPs (Notarianni *et al.*, 2014), depending on embedded positions, i.e. on top of the indium-thin-oxide (ITO) electrode within the hole transport buffer layer (Hwang *et al.*, 2009), (Wu *et al.,* 2011) or within the bulk heterojunction active layer of organic solar cells (Park *et al.*, 2008), (Wang *et al.* 2011a), and various shape of Au-NPs, deposition or blending methods, and coverage densities (Yang *et al.*, 2011), (Shahin *et al.*, 2012), (Chen *et al.*, 2009). However, Jian Wang *et al* (Wang *et al.*, 2016) reported that device performance is significant degradation when active layer P3HT: PCBM is in direct contact with the Au NPs. It was attributed to quenching effect caused by non-radiative energy transfer to Au NPs. Therefore, the separation of Au NPs from the active layer by means of over layer is necessary in order to avoid this exciton quenching and to maximize the device performance. Metal oxides with good electrical characteristics, such as titanium oxide (TiO_2) (Yang *et al.*, 2010) or zinc oxide (ZnO) (Li *et al.*, 2014) can be used as an electron transport layer (ETL) or the separation of Au NPs from the active layer. Among them, ZnO with various nanostructure such as 0 D (nanoparticles), 1D (nanorods, nanofibers, nanowire) 2 D (thin films) is preferred due to its well-aligned bandgap structure of the inverted OSCs and the relativity high electron mobility (Zafar *et al.*, 2020), which increase the transport of electronics from photoactive layer to cathode lead to increase PCE of the inverted OSCs. Hau *et al* (Hau *et al.*, 2008) using a thin layer of ZnO NPs (50 nm) or the ZnO thin films deposited by sol-gel method for the ETL of the inverted OSCs giving the average PCE of 3.6% and 3.5 %, respectively. Zafar *et al* (Zafar *et al.*, 2017) reported the high-density ZnO NR structures are interested in the ETL of the inverted OSCs to enhance electro collection capability by reducing the interface between the photoactive materials and cathode. However, the PCE of the OSCs was low (1.67%), which due to the non-uniform coating of the photoactive material within the deep valleys between NRs. In this work, to further enhance the PCE of organic solar cells, we fabricated the inverted OSCs with structure including glass / ITO / Au NPs / ZnO NR / P3HT: PCBM / PEDOT: PSS / Ag layers (Fig 1). The combination of Au NPs enhances light absorption at the photoactive layer and controls the density of ZnO NR.

2. Materials and Methods

2.1 Device Fabrication

In this study, inverted ZnO NRs/organic solar cells with embedded of Au NPS were fabricated on indium tin oxide (ITO) coated glass substrate (20Ω/sq, Sigma-Aldrich) includes four steps as shown in **Fig. 1**:

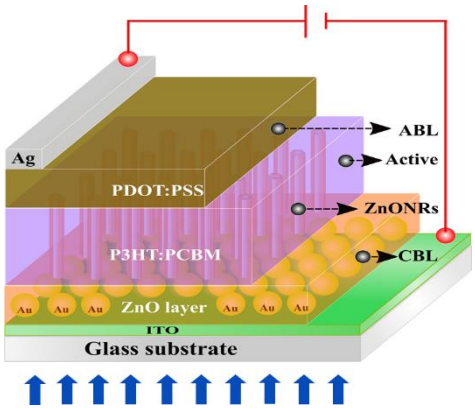

Fig. 1. A schematic diagram of inverted ZnONRs/organic solar cells with inserting Au NPs.

2.2. The preparation of Au NPs.

The substrate was cleaned in an ultrasonic bath using aqueous solution of water, ethanol and acetone (1:1:1) at 80 °C for 5 min, shining under UV-ozone for 10 min. Then, 5 nm thick Au layer was deposited on this substrate using electron beam evaporation, followed by rapid thermal annealing at 300°C to form Au NPs via melting and condensation. During the annealing process, argon was used as a carrier gas to avoid an increase in the sheet resistance of the ITO substrate.

2.3. The preparation of ZnO nanorod.

The ZnO cathode buffer layer (CBL) was synthesized using hydrothermal method following the previous study (Cuong *et al*., 2010). After coated sample with an ethanolic solution of 5 mM zinc acetate dehydrate (98%, Aldrich), the sample was cleaned with ethanol and dried with inert gas. This coating step was repeated five times, followed by thermal annealing at 300°C in argon ambient for 30 min to form the ZnO CBL. Subsequently, the prepared sample was vertically loaded in a 100 mL aqueous solution of 0.016 M zinc nitrate hexahydrate and 0.025 M methylamine. To form ZnONRs, the aqueous solution was heated to 90°C in an oven for 1h. The substrate covered with the ZnO NRs was then cleaned with water and blown with an argon stream.

2.4. The preparation of the active layer and anode buffer layer.

The active material is a mixture of PCBM (electron acceptor) and P3HT (donor material). P3HT and PCBM were dissolved separately in dichlorobenzene with 10 w/v % before mixed with accurately weighted ratio of 1:1, and spin-coated on top of ZnO NRs/Au NPs/ITO substrate at 2000 rpm for 20 s. Prepared sample was dried slowly in the glove-box for 45 min at 140ºC. To prepare PEDOT: PSS anode buffer layer (ABL), the PEDOT: PSS materials was diluted 1:1 with distilled water and passed through a 0.45 µm *polyvinylidene difluoride* (PVDF) membrane filter and then spin-coated at 8000 rpm. In order to dry PEDOT: PSS film, the substrates were baked at 175ºC for 10 min in argon filled glove-box with humidity level lower than 0.5 ppm.

2.5. The preparation of the anode electrode

Finally, 100 nm thick Ag as anode electrode was deposited on top using thermal evaporation to complete photovoltaic device fabrication process.

2.6. Materials and Device Characteristics

The optical property of Au NPs was measured with a UV-Vis spectrophotometer (Hewlett Packard 8453) using the normal incident transmittance. The crystal structure of the samples was characterized using field emission scanning electron microscopy (FE-SEM, JEOL, JSM-600F) and high-resolution X-ray diffraction (HRXRD, Bruker D8 Advance), respectively. The photocurrent was measured by recording the photocurrent density versus voltage (J-V) curve under illumination from a solar light simulator (AM 1.5 with a power density of 100 mW/cm^2, EXIL-0.5850KSVI).

3. Result and Discussion

Figure 2(a) shows the SEM image of Au-NPs formed on ITO coated glass. The diameter of Au-NPs was distributed at around 15~50 nm, observed from the inset SEM image of Fig. 2(a). The absorbance spectrum of bare ITO coated glass and extinction spectrum of the Au-NPs, determined using ultraviolet-to-visible spectroscopy, were displayed in Fig. 2(b). Although the absorption value of ITO coated glass is lower than 20% in the visible range, the ITO films had an opaque window at over ~400 nm ultraviolet (UV) wavelength due to strong absorption at the band gap energy of crystallizing ITO, which is the limitation of ITO materials in field of application of PVs devices for harvesting UV solar energy. The maximum transmittance band of ITO film shows at ~550 nm wavelength. The extinction spectrum of Au-NPs which is calculated via subtracting a reference optical absorption of ITO coated glass shows in Fig. 2(b).

UV-Vis spectrum of prepared Au NPs on ITO film shows a maximum absorbance peak at 550 nm. This value was used to determine the particle size (Eq 1).

$$d(\text{nm}) = \frac{\ln\left(\frac{\lambda spr-\lambda_0}{L_1}\right)}{L_2} \quad (1)$$

where λ_0 = 512 nm; L_1 = 6.53 nm; L_2 = 0.0216 nm^{-1} are parameters determined from the theoretical model, while λ_{spr} is the wavelength in nm that corresponds to the maximum absorbance peak obtained from the UV-Vis spectra.

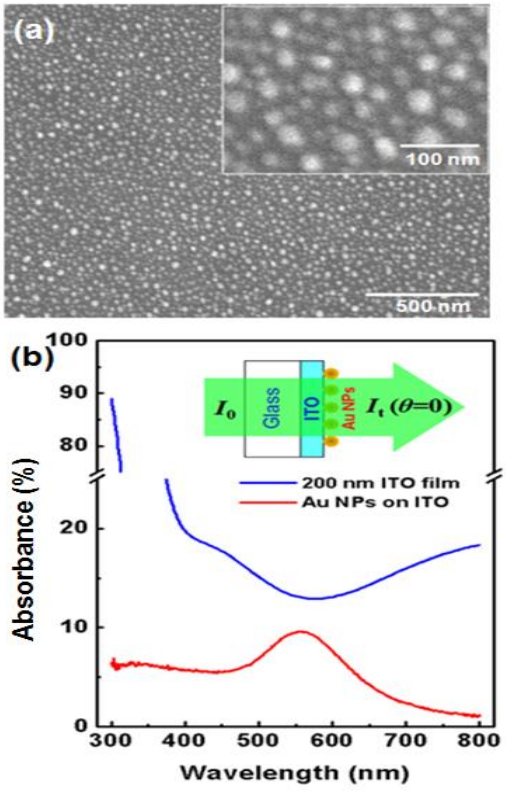

Fig. 2. (a)Top view scanning electron microscope images of Au-NPs formed on ITO coated glass by metal evaporation deposition and thermal annealing. (b) UV-visible absorption spectrum of ITO coated glass and the extinction spectrum of Au-NPs which is calculated via subtracting a reference optical absorption of ITO.

In this way, the diameter size of Au NPs is calculated to be 80 nm that is significantly larger than the observed value from the SEM image. This result is probably associated with the fact that the rapid thermal annealing process usually leads to non-uniformity size because the particles size and shape are very sensitive to the amount of Au deposited on the surface, the annealing temperature and the surface conditions of the ITO substrate. The excitation of LSPs of Au-NPs can be achieved when the frequency of the incident light matches its resonance peak, resulting in unique optical properties; selective light extinction as well as local enhancement of electromagnetic field near the surface of Au-NPs. The resonance peak of LSPs depends strongly on the size, shape, and the dielectric environment of the Au-NPs. The plasmonic resonance regime of the Au-NPs was close to the absorption peak of the P3HT/PCBM blends, thereby suggesting enhanced light-harvesting efficiency of active layer.

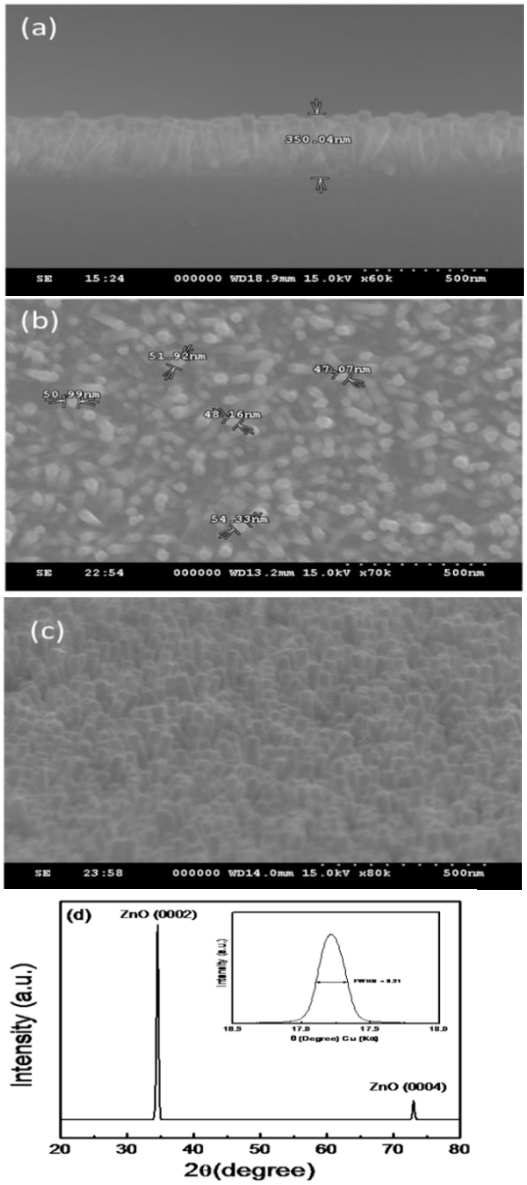

Fig. 3. SEM analysis of hydrothermal growth ZnONRs arrays (a) cross section, (b) top view, (c) bird-view, and (d) The HRXRD diffraction pattern of as-grown ZnONRs.

The FE-SEM images of the as-grown ZnO NRs were shown in Figs. 3(a-c). It illustrates the growth of vertical arrays 350 nm-height ZnO NRs using solution-based method. The diameter of the rods can be observed from the Fig. 3(b) which was about 50 ± 5 nm. The aspect ratio (height divided by diameter) was 7. The bird-view of this dense vertical array ZnO NRs was shown in Fig. 3(c). The crystal structure and orientation of the as-grown ZnO NRs were also characterized using HRXRD measurement as shown in Fig. 3(d). We observe two dominant peaks at 34.45° and 72.59°, referred to the ZnO (002) and ZnO (004) planes, respectively. It indicates that the surface of ZnO NRs is (002) oriented. The inset of Fig. 3(d) shows the XRD θ rocking curve for a peak at 34.35°, with a full width at half-maximum (FWHM) value of 0.21°. The small FWHM value indicates good alignment among different (002) oriented domains of the as-grown ZnO NRs.

Figure 4(a) shows the photocurrent density (*J*) plotted with respect to effective bias (*V*) for the device with and without Au-NPs incorporated, recorded at 100 mW/cm (air mass 1.5G) illuminations. Table 1 shows the open circuit voltage (V_{oc}), short circuit current (J_{sc}), fill factor (FF) and power conversion efficiency (PCE) of inverted ZnO NRs/organic solar cells with and without Au-NPs LSPs effects, as obtained from the *J-V* characteristics under white light illumination. The reference device with the structure ITO/ZnO NRs/P3HT:PCBM/PEDOT:PSS/Ag exhibited characteristics for V_{oc} of 0.55 V, J_{sc} of 6.9 mA/cm², and FF of 51.0%, resulting in PCE of 2.4%. The LSPs effects of Au-NPs incorporated on device performance is obviously determined.

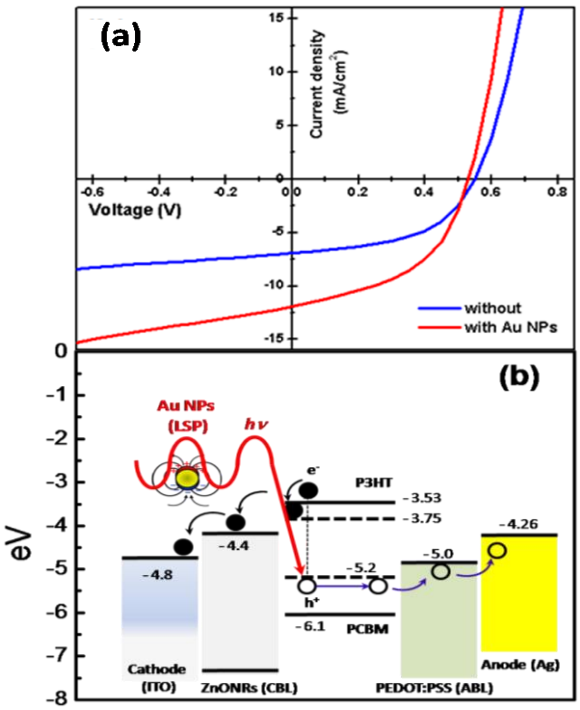

Fig. 4. (a) Photocurrent density (*J*) plotted with respect to effective bias (*V*) for the reference and Au-NPs plasmonic devices, (b) the architecture band diagrams for systematically explored plasmonic effects of the device characteristics of P3HT/PCBM based organic solar cells.

Table 1
Photovoltaics characteristics of the plasmonic organic solar cells incorporating Au-NPs between ITO and ZnO cathode buffer layer. The table shows the optimized cell performance for each size.

Cell device	J_{sc} (mA/cm^2)	V_{oc} (V)	FF (%)	PCE (%)	Enhancement (%)
Ref. device	6.9	0.55	51	2.4	
AuNPs incorporated device	12	0.53	48	3.8	58

When the Au-NPs were inserted, the device shows higher value of J_{sc} (12 mA/cm^2) although the fill factor slightly decreased. The calculated PCE is clearly higher as 3.8 %. The PCE value significantly increased 58 % which clearly shows the enhancement effect the absorption of solar energy through LSPs effects of incorporated Au-NPs. The schematic diagram of the energy levels and the transport directions of electrons and holes in an inverted ZnO NRs/organic hybrid solar cell are illustrated in Fig. 4(b). It should be noted that inserting Au NPs have both advantage and disavantage effect on device performances. Herein, Au NPs are fovorable to LSPs in coupling of scattered light from ZnO NRs to increase the light's path length in the absorbing medium. Although the light absorption in the active layer can be enhanced, Au NPs may also act as recombination centers within the active layer. To avoid this adverse effect, Au NPs are covered by the ZnO seeded-layer to prevent Au NPs from direct contact with the active layer. Moreover, ZnO seeded layer also facilitates to grow vertical ZnO NRs arrays, which function as a CBL in inverted device structure as follows: (i) the conduction band bottom of ZnO NRs is around -4.4 eV, which allows it to collect electrons and block holes, impedes the charge recombination, (ii) the band edge cut-off of ZnO NRs at around 375 nm can block UV light and accordingly prevent the organic active materials degradation under UV light irradiation. Overall, the enhanced efficiency of inverted ZnO NRs/organic hybrid solar cells arises from an enhancement of the light absorption in the active medium due to Au NPs and suppressing charge recombination due to ZnO CBL.

Figure 5(a) presents IPCE curves for these devices. We also compared the curve of the differential ratio of IPCE (ΔIPCE) after incorporating Au NPs with the extinction spectrum of the Au NPs as shown in Figure 5(b). Au NPs incorporated cells has higher value of IPCE, especially in the absorption energy range from 1.9 eV to 2.4 eV. This energy regime coincides with the extinction range of the Au-NPs, indicating that LSPs resonance effects did indeed improve the photocurrent. The LSPs resonance induced by the Au-NPs not only increased the degree of light absorption but also enhanced the degree of exciton dissociation. As a result, the photocurrent and overall device efficiency were both improved considerably after exploiting the optical effects of the LSPs resonance. However, to explore the LSPs resonance effects on the exciton generation behavior, we have to understand the interplay between the LSPs in Au-NPs and the generated excitons in active layer by solar energy absorption. Thereby, there are considered that the steady-state carrier dynamics between exciton dissociation and recombination process mechanisms. Firstly, the most of excited electrons from HOMO level to LUMO level formed bounded or free excitons before dissociation and sweeping by implied bias of PVs cells. These excitons interacted with self sustained LSPs in Au-NPs and formed the plasmon-exciton coupled modes. The results of plasmon-exciton coupling enhanced not only the rate of exciton dissociation but also the exciton recombination via radiative and/or non-radiative processes accorded strong electric field oscillation. In particular, the radiative recombination processes are re-emitting to free space and reduced the photocurrent as investigating of photoluminescence enhanced effects of metallic plasmon incorporated organic solar active films in previous reported works (Shahin *et al*., 2012), (Chen *et al.*, 2009), (Chen *et al*., 2013),(Wang *et al.* 2011b). Accordingly, it was believed that the dip valleys of ΔIPCE spectrum at 2.30 eV and 2.35 eV in Fig. 5(b) are corresponded to bounded and free excitons in active layer, which has HOMO-to-LUMO inter-level transition energy of 2.35 eV and suggested exciton binding energy of ~50 meV, respectively. The luminous recombination process is dependent on the light excitation rate and the quantum yield, which is dependent on competition between the radiative and non-radiative decaying mechanisms.

.

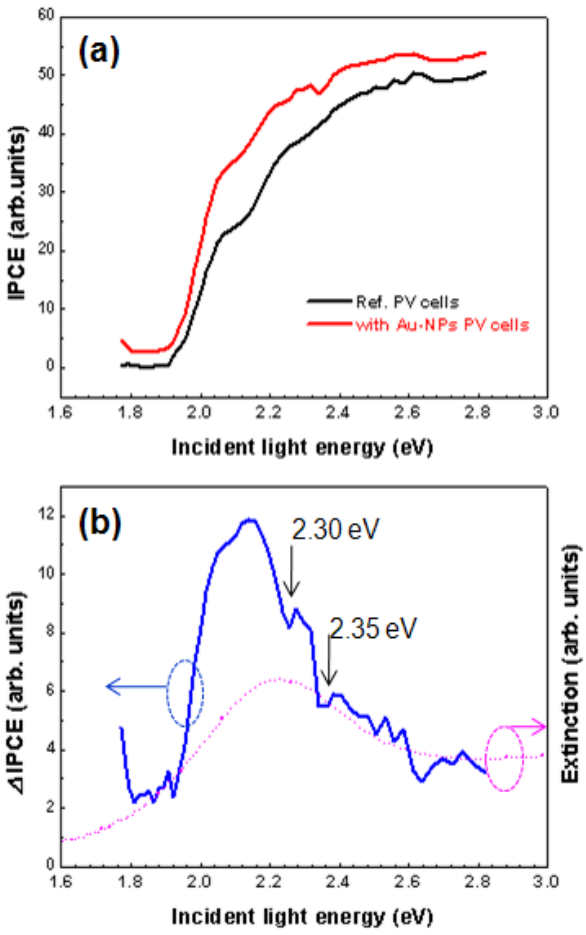

Fig. 5. (a) Corresponding IPCE curves of the reference and Au-NPs plasmonic organic PVs devices. (b) Comparison between the curve of the increase in IPCE (ΔIPCE) after incorporating Au NPs and the extinction spectrum of the Au NPs

Because the LSPs resonance frequency of Au-NPs was exactly close to the absorption band of P3HT:PCBM and both the non-radiative decay processes and thermally energy relaxation of electron in inner LUMO levels are more dominant, we attribute the PCE losses due to the radiative decay is negligible, compared with the increasing of absorption rate and enhancement factor of light excitation. Therefore, the LSPs resonance effects, induced by the presence of the Au-NPs, enhanced light collection in the active layer of organic PVs predominately through local field enhancement.

4. Conclusion

In summary, we improved the PCEs of inverted ZnO NRs/organic solar cells by incorporating Au-NPs between ITO and the ZnO NRs cathode buffer layer. The PCEs enhancement effect occurs in the spectral region that coincident with the Au-NPs plasmon extinction band. The degree of light absorption in the plasmonic-enhanced organic solar cells increased significantly as a result of LSPs resonance induced local field enhancement. Moreover, interactions between the plasmons and the photo-generated excitons resulted in an enhanced degree of exciton dissociation.

Acknowledgments

This research was funded by the Vietnam National Foundation for Science and Technology Development (NAFOSTED) under grant number 103.02-2018.352

Conflicts of Interest: The authors declare no conflict of interest.

References

Alem, S., Bettignies, R. De, Nunzi, J., & Cariou, M. (2004). Efficient polymer-based interpenetrated network photovoltaic cells. *Applied Physics Letters*, *84*(12), 2178–2180. https://doi.org/10.1063/1.1669065

Alem, S., Gao, J., Wantz, G., Alem, S., Gao, J., & Wantz, G. (2013). Photovoltaic response of symmetric sandwich polymer cells with identical electrodes Photovoltaic response of symmetric sandwich polymer cells with identical. *Journal of Applied Physics*, *044505*(2009). https://doi.org/10.1063/1.3200954

Ameri, T., Dennler, G., Lungenschmied, C., & Brabec, C. J. (2009). Organic tandem solar cells : A review. *Energy & Environmental Science*, 347–363. https://doi.org/10.1039/b817952b

Brabec, C. J., Shaheen, S. E., Winder, C., Sariciftci, N. S., & Denk, P. (2002). Effect of LiF/metal electrodes on the performance of plastic solar cells. *Applied Physics Letters*, *80*(7), 1288–1290. https://doi.org/10.1063/1.1446988

Chen, F., Wu, J., Lee, C., Hong, Y., Kuo, C., & Huang, M. H. (2009). Plasmonic-enhanced polymer photovoltaic devices incorporating solution-processable metal nanoparticles. *Applied Physics Letters*, *95*(013305), 1–5. https://doi.org/10.1063/1.3174914

Chen, X., Zuo, L., Fu, W., Yan, Q., Fan, C., & Chen, H. (2013). Solar Energy Materials & Solar Cells Insight into the efficiency enhancement of polymer solar cells by incorporating gold nanoparticles. *Solar Energy Materials and Solar Cells*, *111*, 1–8. https://doi.org/10.1016/j.solmat.2012.12.016

Cuong, T. V., Pham, V. H., Chung, J. S., Shin, E. W., Yoo, D. H., Hahn, S. H., Huh, J. S., Rue, G. H., Kim, E. J., Hur, S. H., & Kohl, P. A. (2010). Solution-processed ZnO-chemically converted graphene gas sensor. *Materials Letters*, *64*(22), 2479–2482. https://doi.org/10.1016/j.matlet.2010.08.027

Eo, Y. S., Rhee, H. W., Chin, B. D., & Yu, J. W. (2009). Influence of metal cathode for organic photovoltaic device performance. *Synthetic Metals*, *159*(17–18), 1910–1913. https://doi.org/10.1016/j.synthmet.2009.05.036

Green, M. A., Emery, K., Hishikawa, Y., Warta, W., & Dunlop, E. D. (2014). *Solar cell ef fi ciency tables (version 44). version 44*, 701–710. https://doi.org/10.1002/pip

Gu, M., Ouyang, Z., Jia, B., Chen, X., Fahim, N., Li, X., Ventura, M. J., & Shi, Z. (2012). Nanoplasmonics : a frontier of photovoltaic solar cells. *Nanopho*, *1*, 235–248. https://doi.org/10.1515/nanoph-2012-0180

Hau, S. K., Yip, H., Baek, N. S., Zou, J., Malley, K. O., Hau, S. K., Yip, H., Baek, N. S., Zou, J., Malley, K. O., & Jen, A. K. (2008). Air-stable inverted flexible polymer solar cells using zinc oxide nanoparticles as an electron selective layer Air-stable inverted flexible polymer solar cells using zinc oxide nanoparticles as an electron selective layer. *Applied Physics Letters*, *92*(253301), 1–4. https://doi.org/10.1063/1.2945281

Hoppe, B. H., Niggemann, M., Winder, C., Kraut, J., Hiesgen, R., Hinsch, A., Meissner, D., & Sariciftci, N. S. (2004). *Nanoscale Morphology of Conjugated Polymer / Fullerene-Based Bulk-Heterojunction Solar Cells **. 10*, 1005–1011. https://doi.org/10.1002/adfm.200305026

Hwang, J., Hwan, J., Soo, J., Yun, D., & Cho, K. (2009). High efficiency polymer solar cells with wet deposited plasmonic gold nanodots. *Organic Electronics*, *10*(3), 416–420. https://doi.org/10.1016/j.orgel.2009.01.004

Jagadeesh, V., Vempati, S., & Sundarrajan, S. (2014). ScienceDirect Effective nanostructured morphologies for efficient hybrid solar cells. *Solar Energy*, *106*, 1–22. https://doi.org/10.1016/j.solener.2013.08.037

Kaltenbrunner, M., White, M. S., Głowacki, E. D., Sekitani, T., Someya, T., Sariciftci, N. S., & Bauer, S. (2012). *ultrathin and lightweight organic solar cells with high flexibility*. https://doi.org/10.1038/ncomms1772

Krebs, F. C. (2009). *Solar Energy Materials & Solar Cells Fabrication and processing of polymer solar cells : A review of printing and coating techniques*. *93*, 394–412. https://doi.org/10.1016/j.solmat.2008.10.004

Li, P., Jiu, T., Tang, G., Wang, G., Li, J., Li, X., & Fang, and J. (2014). Solvents Induced ZnO Nanoparticles Aggregation Associated with Their Interfacial Effect on Organic Solar Cells. *ACS Applied Materials and Interfaces*, *6*(20), 18172–18179. https://doi.org/10.1021/am5051789

Liang, B. Y., Xu, Z., Xia, J., Tsai, S., Wu, Y., Li, G., Ray, C., & Yu, L. (2010). *For the Bright Future — Bulk Heterojunction Polymer Solar Cells with Power Conversion Efficiency of 7 . 4 %*. 135–138. https://doi.org/10.1002/adma.200903528

Lu, L., Luo, Z., Xu, T., & Yu, L. (2012). Cooperative Plasmonic E ff ect of Ag and Au Nanoparticles on Enhancing Performance of Polymer Solar Cells. *Nano Letters*.

Notarianni, M., Vernon, K., Chou, A., Aljada, M., Liu, J., & Motta, N. (2014). ScienceDirect Plasmonic effect of gold nanoparticles in organic solar cells. *Solar Energy*, *106*, 23–37. https://doi.org/10.1016/j.solener.2013.09.026

Park, M., Chin, B. D., Yu, J. W., Chun, M. S., & Han, S. H. (2008). Enhanced photocurrent and efficiency of poly(3-hexylthiophene)/fullerene photovoltaic devices by the incorporation of gold nanoparticles. *Journal of Industrial and Engineering Chemistry*, *14*(3), 382–386. https://doi.org/10.1016/j.jiec.2008.01.014

Shahin, S., Gangopadhyay, P., & Norwood, R. A. (2012). Ultrathin organic bulk heterojunction solar cells : Plasmon enhanced performance using Au nanoparticles. *Applied Physics Letters*, *101*(053109), 1–4.

Tang, Z., Tress, W., & Ingana, O. (2014). *Light trapping in thin film organic solar cells*. *June*. https://doi.org/10.1016/j.mattod.2014.05.008

Wang, D. H., Kim, D. Y., Choi, K. W., Seo, J. H., Im, S. H., Park, J. H., Park, O. O., & Heeger, A. J. (2011a). Enhancement of Donor – Acceptor Polymer Bulk Heterojunction Solar Cell Power Conversion Efficiencies by Addition of Au Nanoparticles **. *Angew.Chem.Int.Ed*, *14*, 5519–5523. https://doi.org/10.1002/anie.201101021

Wang, D. H., Kim, D. Y., Choi, K. W., Seo, J. H., Im, S. H., Park, J. H., Park, O. O., & Heeger, A. J. (2011b). Enhancement of Donor – Acceptor Polymer Bulk Heterojunction Solar Cell Power Conversion Efficiencies by Addition of Au Nanoparticles **. *Angew.Chem.Int.Ed*, *50*, 5519–5523. https://doi.org/10.1002/anie.201101021

Wang, K., Liu, C., Meng, T., Yi, C., & Gong, X. (2016). Inverted organic photovoltaic cells. *Chemical Society Reviews*, *45*(10), 2937–2975. https://doi.org/10.1039/c5cs00831j

Wu, J. L., Chen, F. C., Hsiao, Y. S., Chien, F. C., Chen, P., Kuo, C. H., Huang, M. H., & Hsu, C. S. (2011). Surface plasmonic effects of metallic nanoparticles on the performance of polymer bulk heterojunction solar cells. *ACS Nano*, *5*(2), 959–967. https://doi.org/10.1021/nn102295p

Yang, J., You, J., Chen, C., Hsu, W., Tan, H., & Zhang, X. W. (2011). Plasmonic Polymer Tandem Solar Cell. *ACS Nano*, *5*(8), 6210–6217.

Yang, P., Zhou, X., Cao, G., & Luscombe, C. K. (2010). P3HT:PCBM polymer solar cells with TiO2 nanotube aggregates in the active layer. *Journal of Materials Chemistry*, *20*(13), 2612–2616. https://doi.org/10.1039/b921758d

Yu, G., Gao, J., Hummelen, J. C., Wudl, F., & Heeger, A. J. (2004). Polymer Photovoltaic Cells : Enhanced Efficiencies via a Network of Internal Donor-Acceptor Heterojunctions. *Advanced Functional Materials*, 1789–1791.

Zafar, M., Kim, B., & Kim, D. (2020). Improvement in performance of inverted organic solar cell by rare earth element lanthanum doped ZnO electron buffer layer. *Materials Chemistry and Physics*, *240*(May 2019), 122076. https://doi.org/10.1016/j.matchemphys.2019.122076

Zafar, M., Yun, J., & Kim, D. (2017). Applied Surface Science Performance of inverted polymer solar cells with randomly oriented ZnO nanorods coupled with atomic layer deposited ZnO. *Applied Surface Science*, *398*, 9–14. https://doi.org/10.1016/j.apsusc.2016.11.211